RSC Advances

PAPER

View Article Online
View Journal | View Issue

Cite this: *RSC Adv.*, 2016, **6**, 38201

Multiple-responsive ionic complex luminogen of quinine and camphorsulfonic acid with aggregation-induced emission†

Pei-Yi Huang, Jhen-Yan Gao, Cheng-Yu Song and Jin-Long Hong*

Received 8th January 2016
Accepted 3rd April 2016

DOI: 10.1039/c6ra00603e

www.rsc.org/advances

Bulky camphorsulfonic acid (CSA) was used to complex with quinine (Qu) to impose restricted intramolecular rotation (RIR) required for aggregation-induced emission (AIE) properties. After complexation with two equivalents of CSA, the non-emissive quinine (Qu) base can be protonated to produce an ionic complex $Qu(CSA)_2$ with AIE properties. The ionic bonds in the complex $Qu(CSA)_2$ are sensitive to various external stimuli, which allows its use as a luminescent sensor for pH values and different metal ions. Moreover, the ionic $Qu(CSA)_2$ can be a denaturant and biological sensor for the blood protein of bovine serum albumin (BSA); through the use of $Qu(CSA)_2$, the unfolding process of the BSA chains was evaluated. Theoretical and practical aspects of this ionic $Qu(CSA)_2$ complex are discussed in this study.

Introduction

In 2001, Tang's group discovered the interesting aggregation-induced emission (AIE) properties of the propeller-shaped molecule of 1-methyl-1,2,3,4,5-pentaphenylsilole (MPS)[1,2] and that MPS emits strongly in the aggregated and the solid states despite being non-emissive in a dilute solution. The discovery of MPS thereafter inspired further research for a wide variety of organic and polymeric luminogens with the advanced AIE properties.[3–11] Just like MPS, most AIE-active luminogens (AIEgens) are propeller-shaped with restricted intramolecular rotation (RIR)[12,13] as the inherent mechanism responsible for the AIE property. Taking MPS as an example, the rotation of the phenyl rotors of MPS is hampered in the aggregated state due to steric shielding from neighboring propellers, thus blocking the non-radiative decay pathways to result in strong emission. New AIEgens restricted in molecular rotation were therefore designed, prepared, and explored for their potential as functional materials[3–11] such as sensors for chemicals, explosives, pH value, proteins, DNAs and RNAs, and as emitting layer for OLEDs and PV cells.

Since the early discovery from the bark of the cinchona (quinine-quina) tree in the 1600 s, quinine remains as an important anti-malarial drug[14] for almost 400 years. Besides being a cure for malaria, quinine is also a stable luminogen in its acidic solution form, and quinine base in aqueous H_2SO_4 (0.1 N) was constantly used as a standard for calibrating solution quantum yield[15–17] of various luminogens. Therefore, the photophysical behavior of quinine sulfate in a homogenous medium[18,19] has been studied extensively. In addition, luminescence of quinine sulfate was reported to be quenched by halides, and halide ions,[20–22] which provided valuable methodology in the detection of hazardous chemicals in a physical chemistry laboratory.

The quinine molecule possesses the chemical structure of two heterocyclic quinoline and quinuclidine rings connected by two rotatable chemical bonds (bonds 1 and 2 in Scheme 1). It was then conceivable to us that the quinine molecule is a potential AIEgen if its rotatable bonds can be effectively restricted by known chemical or physical methods. The protonation sites of the two nitrogen atoms in the respective quinoline and quinuclidine rings provided a readily available pathway to impose the required rotational restriction for quinine; that is, by protonating the two nitrogen atoms with a bulky acid, such as camphorsulfonic acid (CSA), we easily

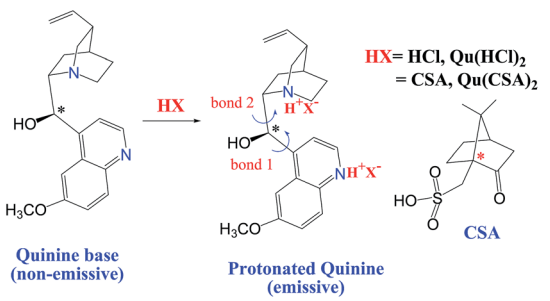

Scheme 1 Protonations of non-emissive quinine base to emissive, ionic complex of $Qu(HX)_2$.

Department of Materials and Optoelectronic Science, National Sun Yat-sen University, Kaohsiung 80424, Taiwan, Republic of China. E-mail: jlhong@mail.nsysu.edu.tw

† Electronic supplementary information (ESI) available. See DOI: 10.1039/c6ra00603e

made the resultant complex $Qu(CSA)_2$ a novel AIEgen. Using CSA to impose RIR for AIEgens had been previously conducted in our laboratory, where the small-molecule 2,4-diphenylquinoline (DPQ) and poly(vinyl2,4-enylquinoline) (PVQ)[23] were separately complexed with equivalent amounts of CSA and the resultant DPQ-CSA and PVQ-CSA complexes were shown to exhibit higher emission intensity than the respective precursors of DPQ and PVQ. We therefore applied the same methodology to quinine; however, the result is more meaningful considering that CSA complexation actually converted the non-emissive quinine base into a highly-emissive one with the desired AIE activity. The ionic bonds sustaining AIE activity of the $Qu(CSA)_2$ complex are also rather sensitive to various additives according to our experimental results and thus, under the operations of acid, base, metal ions, and natural protein of bovine serum albumin (BSA), ionic bonds connecting the bulky CSAs will be ruptured and result in a non-emissive quinine molecule without any AIE activity. The inherent ionic bonds therefore made the ionic complex of $Qu(CSA)_2$ a multiple luminescent sensor towards various external additives. The AIE character of $Qu(CSA)_2$ and its further use as luminescent sensor are discussed here.

Experimental section

Materials

Quinine (Alfa Aesar, 99% base) and D(+)-10-camphorsulfonic acid (Acros) were used directly without further purification. BSA (Sigma) was stored in a refrigerator before use. Ionic complexes were prepared according to the procedures given below:

Preparation of $Qu(CSA)_2$ complex. Quinine (1 mmol, 324 mg) was mixed with CSA (2 mmol, 464 mg) in deionized water (10 mL). The resulting solution was then stirred vigorously under nitrogen atmosphere for one day to ensure complete reaction. Deionized water was then removed by rotary evaporation at 90 °C, followed by vacuum distillation at 80 °C for one day to obtain the solid $Qu(CSA)_2$ complex.

Preparation of $Qu(HCl)_2$ complex. HCl (2 mmol, 0.16 mL) solution was dropped slowly into a solution of quinine (1 mmol, 324 mg) in deionized water (10 mL) with vigorous stirring. The resulting solution was stirred at room temperature under nitrogen atmosphere for another day before rotary evaporation at 90 °C to remove water. The resulting solid was vacuum dried at 80 °C for one day to obtain the final solid complex of $Qu(HCl)_2$.

Instrumentation

The ^1H NMR spectra were recorded with a Varian VXR-500 MHz instrument. UV-vis absorption spectra were recorded with an Ocean Optics DT 1000 CE 376 spectrophotometer. Emission spectra were obtained from a LabGuide X350 fluorescence spectrophotometer using a 450W Xe lamp as the continuous light source. A small quartz cell with dimensions 0.2 × 1.0 × 4.5 cm^3 was used for the absorption and emission spectra to reduce potential inner filter effects. Particle sizes in selective solvent pairs were measured by a dynamic light scattering instrument (DLS) on a Brookhaven 90 plus spectrometer at room temperature; an argon ion laser operating at 658 nm was used as the light source. Circular dichroism spectra were recorded using a JASCO J-810 spectrometer.

Results and discussion

The essential role of bulky CSA in generating AIE properties of the quinine complex can be demonstrated by the varied emission behavior between complexes of $Qu(CSA)_2$ and $Qu(HCl)_2$. Without bulky CSA to inherit hindered rotation, $Qu(HCl)_2$ just behaved like traditional luminogens with aggregation-caused quenching (ACQ) properties,[24] in that the solution emission decreased with increasing luminogen concentration (Fig. 1A). Aggregates formed in a concentrated solution are therefore detrimental to the emission of $Qu(HCl)_2$. An analogous complex of $Qu(H_2SO_4)_2$ also behaved with typical ACQ properties according to its solution emission spectra at different concentrations (Fig. S4†).

In contrast, $Qu(CSA)_2$ is a typical AIEgen with more intense emissions in more concentrated solutions (Fig. 1B). A dilute solution (10^{-5} M) of $Qu(CSA)_2$ is non-emissive but increasing concentration drastically increased the solution emission.

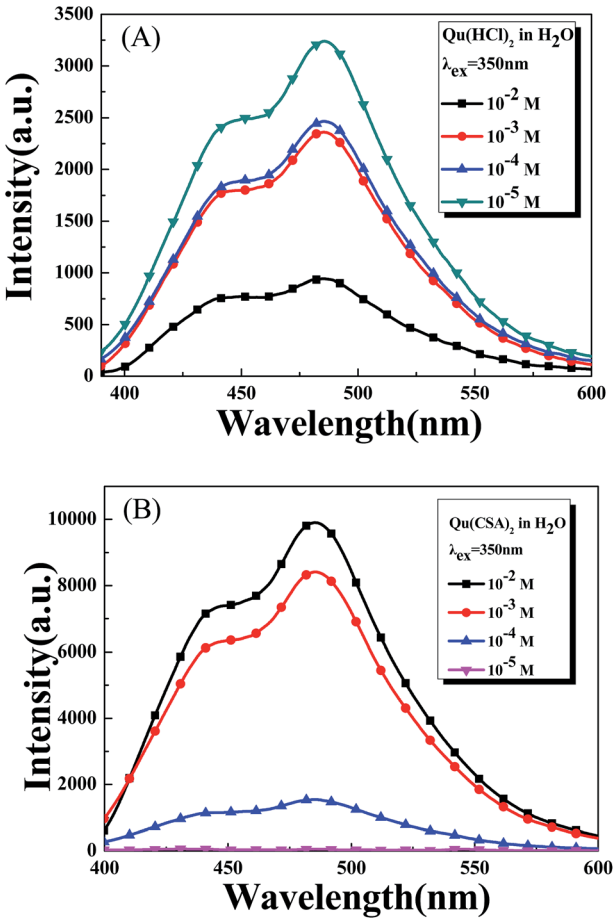

Fig. 1 Emission spectra of the aqueous solutions of (A) $Qu(HCl)_2$ and (B) $Qu(CSA)_2$ at different concentrations from 10^{-5} to 10^{-2} M.

Aggregates formed in the concentrated solution are supposed to be higher in emission than the more isolated species in the dilute solution, which is the typical behavior of AIEgens. Emission spectra of $Qu(CSA)_2$ contain two overlapping bands with the short- and long-wavelength emissions being those of the monomer and aggregate emission, respectively. With increasing solution concentration, the aggregate emission largely raised its contribution to the whole emission compared to that of the monomeric species, which demonstrates that aggregates formed in a concentrated solution are beneficial for the solution emission. Rotational restriction imposed by the bulky CSA is responsible for the resultant AIE activity of $Qu(CSA)_2$; without assistance of the bulky component, complexes of $Qu(HCl)_2$ and $Qu(H_2SO_4)_2$ just behaved like traditional luminogens for which concentration attenuates solution emission.

We may also emphasize the role of CSA by its quantity in the complex as we inspected the solution emission (Fig. 2A) of complexes $Qu(CSA)_x$ containing different amounts of CSA: with less CSA (*i.e.* $x = 0.5$), the corresponding complex solution emitted dimly but increasing CSA content to a higher value of $x = 1$ and 2 significantly raised the emission intensity. Beyond the stoichiometric amount of CSA (*i.e.* $x = 2$), further CSA loading contributed little to emission intensity of the complex solutions, which indicates that the complexation reaction between nitrogen atoms of quinine and sulfonic acids of CSA proceeded quantitatively resulting in ionic complexes containing stoichiometric amounts of quinine and CSA loaded in the solutions. The ionic complex of $Qu(CSA)_2$ was selected for further study here.

The AIE character of $Qu(CSA)_2$ was identified by the standard approach using non-solvent conditions to induce aggregates in the solution for study. A pure solution of $Qu(CSA)_2$ in the good solvent of THF is weak (Fig. 2B) in emission and increasing hexane (bad solvent) fraction from 20 vol% to 80 vol% progressively raised the emission intensity of the mixture solutions as anticipated. The most drastic emission gain was with the solution containing 80 vol% of hexane, wherein the aggregates formed emitted with an intensity at least twice that in solution with less hexane. Aggregate formation was also reflected in the enlarged aggregate emission in the solution containing more hexane non-solvent. Thus, we can easily identify the AIE character of $Qu(CSA)_2$.

The rotational restriction imposed by CSA can be identified by investigating ^{1}H NMR spectra of the $Qu(CSA)_x$ complexes. As reported previously,[25] the ^{1}H NMR peak shape analysis is a powerful tool for characterizing hampered bond rotation based on the observation that fast conformational changes caused by fast molecular rotations result in sharp resonance peaks, whereas slower changes due to restricted molecular rotation broaden the resonance peaks. In many polymeric AIEgens[26,27] the rotational restriction imposed by high MW polymers is so effective that the corresponding resonance peaks weakened in intensity or even disappeared. To understand the effect of CSA, we loaded different amounts of it in solution with constant quinine concentration (10^{-3} M) and the resultant solutions were then subjected to NMR analysis (Fig. 3) in selected ranges corresponding to resonances of the quinine unit in the complexes. With increasing CSA in solution, most of

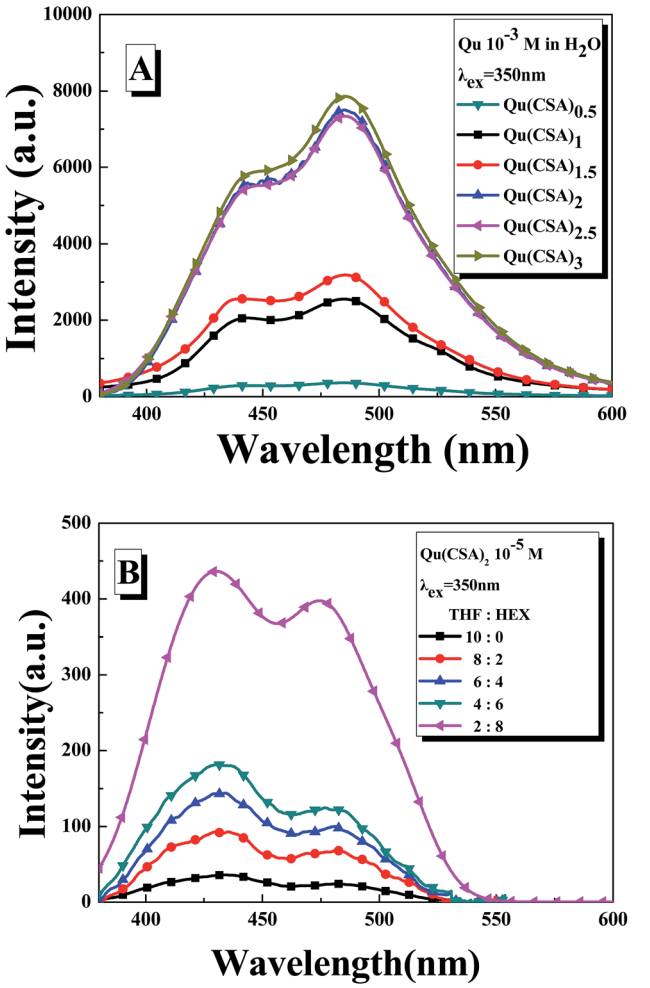

Fig. 2 Emission spectra of (A) quinine (10^{-3} M) in the presence of different amounts of CSA and (B) $Qu(CSA)_2$ in THF/hexane mixture of different volumetric ratios.

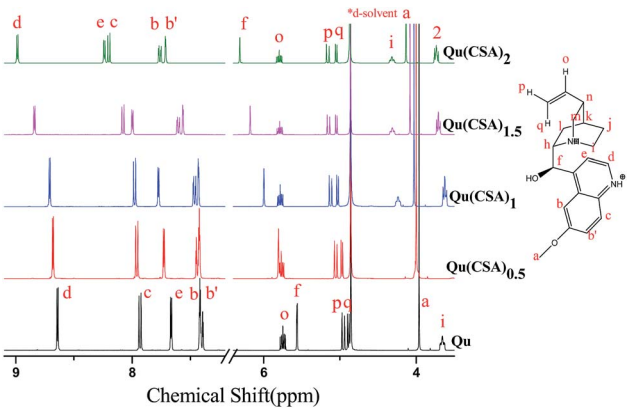

Fig. 3 ^{1}H NMR spectra of $Qu(CSA)_x$ (x: molar ratio of CSA relative to quinine) in the selected ranges from 4 to 9 ppm (CD_3OD).

the resonance peaks gradually shifted downfield, which correlates with the electron-deficiency caused by the CSA protonation. Besides the downfield shift, a more important feature in Fig. 3 is the gradual integration reduction with some resonance peaks of the quinine moiety with increasing CSA content in the NMR solution. The quinoline resonances of protons $H_{b,b',c,d,e}$, and the resonance of proton H_f connected to the carbon atoms of the rotatable bonds exhibited gradual peak reduction with increasing CSA content in the solution. Because all the spectra were conducted with a constant amount of quinine, weakening of the resonance peaks must be due to increasing rotation difficulty in the frozen quinine moiety with incorporated CSA. The protons attached to the frozen bonds are slow in responding to external magnetic stimuli. The more that CSA molecules are added in the NMR tubes, the less intense the resonance peaks are resolved in the corresponding NMR spectra. Therefore, the bulky CSA is an efficient rotation blocker, acting to restrict the motion of the quinine rings and resulting in the desired AIE-related emission.

$Qu(CSA)_2$ as sensor for acid and base

Under the operation of acid and base, the ionic bonds of $Qu(CSA)_2$ can be easily ruptured to result in species of varied emission efficiency; therefore, $Qu(CSA)_2$ is a good luminescence sensor toward acid and base. Emission spectra of $Qu(CSA)_2$ ($= 10^{-3}$ M) in aqueous solutions of different pH values were then measured and the summarized results (Fig. 4) suggest that adding acid (HCl) and base (NaOH) all resulted in emission reduction; however, the reactions leading to the observed emission reduction are not the same.

For the acid-catalyzed reaction, the ionic bonds of $Qu(CSA)_2$ were dissociated by HCl resulting in the protonated quinine complex of $Qu(HCl)_x$ and CSA. Lowering emission intensity in the acidic solution is attributed to the generation of $Qu(HCl)_x$ species, which emitted with less emission efficiency than the initial $Qu(CSA)_2$. A more acidic environment resulted in more of less emissive $Qu(HCl)_x$, therefore reducing the emission intensity to a lower value. At pH 1, the solution emission is low but still discernible, but for the alkaline condition complete emission quenching can be readily achieved. In contrast to HCl, KOH base added in the alkaline solution directly converted the emissive $Qu(CSA)_2$ into the non-emissive quinine base, which should lead to fast emission quenching in the alkaline solution. Formation of non-emissive quinine base is therefore responsible for the large emission reduction at pH 9 and the complete emission quenching at pH 11. The ionic bonds of $Qu(CSA)_2$ are therefore pretty sensitive to acid and base.

Emission response towards metal salts

In the presence of an equivalent amount of metal salt, $Qu(CSA)_2$ (10^{-3} M) emitted (Fig. 5) with an intensity lower than that of pure $Qu(CSA)_2$. In essence, the counter anion dissociated from metal ion is responsible for the reduced emission observed in Fig. 5. To specify the effect of a counter anion, three sets of metal salts with the respective Mg, Cu, and Ca metal ions bound by two different counter anions were used in the experiments. The results suggested that the smaller counter anion (*i.e.* Cl^-) is easier to displace/exchange with the bulky CSA ligand of $Qu(CSA)_2$, rendering larger emission reduction than larger anions (*i.e.*, SO_4^{2-}, CH_3COO^- or OH^-). $Qu(CSA)_2$ is therefore a luminescent sensor for the counter anions of metal salts.

Bovine serum albumin-driven emission variations

Among varieties of serum albumin, bovine serum albumin (BSA)[27] is the commonly studied one in biochemistry or biomedical science due to its structural similarity with human serum albumin (HSA).[28] As a large globular protein (66 kDa) consisting of 583 amino acid residues in a single polypeptide chain, BSA was often used as a binding material with certain dyes and probes, which provided information regarding binding mechanisms.[29] As was reported[30] previously, BSA contains two main fluorescent tryptophan units, Trp-212 and Tyr-263, and the emission of BSA at 350 nm provided useful information regarding conformational changes around the hydrophobic domain containing Trp-212. The indole group of Trp residues in protein is sensitive to surrounding

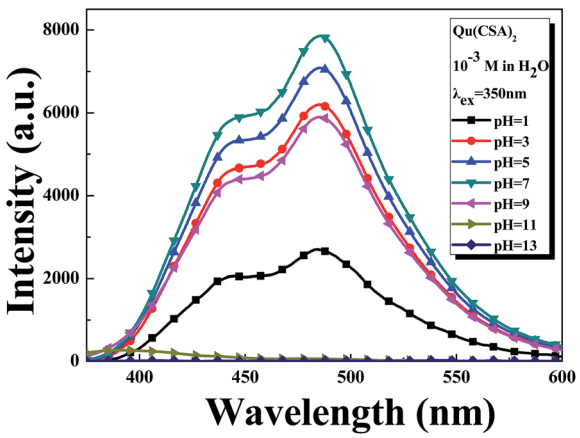

Fig. 4 Emission spectra of the $Qu(CSA)_2$ in the aqueous solutions of different pHs. ($[Qu(CSA)_2] = 10^{-3}$ M, $\lambda_{ex} = 350$ nm).

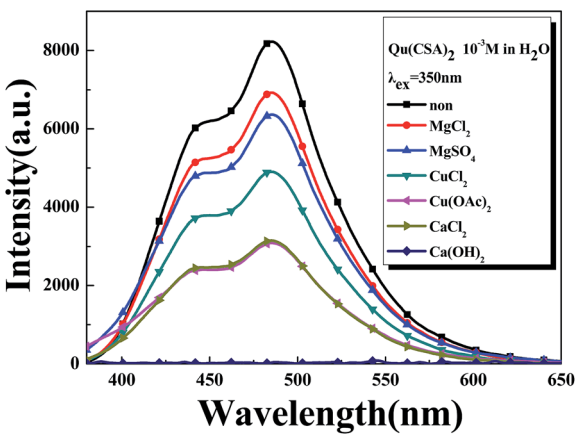

Fig. 5 Emission spectra of $Qu(CSA)_2$ (10^{-3} M) in the presence of different metal salts (10^{-3} M).

environment, and the emission spectra of the indole provide information regarding the environment surrounding the Trp residue. The emission from an exposed surface is known to occur at longer wavelengths than that from a Trp residue in the interior region of protein.

Several ionic compounds, such as guanidinium chloride (GndHCl),[31,32] cationic and anionic surfactants,[33–35] or ionic liquid,[36] had been employed previously as denaturant to uncoil the folded chain of proteins. Several luminescent dyes[37–42] were further applied for investigating the unfolding process of protein induced by the ionic denaturant. One example related to the use of AIEgen[42] (*i.e.* sodium 1,2-bis[4-(3-sulfonatopropoxyl) phenyl]-1,2-diphenylethene (BSPOTPE)) as a luminescent sensor to evaluate the unfolding process of HSA induced by GndHCl. Utilizing the AIE feature of BSOPTPE and the Förster resonance energy transfer from Trp of HSA to BSPOTPE, the unfolding process of HSA induced by GndHCl was monitored and a multistep transition with the involvement of molten globule was proposed to account for the luminescent response in aqueous solutions of HSA and BSPOTPE containing different amounts of GndHCl.

In contrast to the use of extra denaturant in a previous study,[31–42] a simpler recipe involving only $Qu(CSA)_2$ and BSA was used in the present study for investigation of the unfolding process of the peptide chain since we found that the ionic $Qu(CSA)_2$, by itself, is already an effective denaturant capable of uncoiling the folded chain of BSA. By monitoring the emission variation of BSA and $Qu(CSA)_2$, the unfolding process of BSA during the $Qu(CSA)_2$-induced denaturation can be successfully monitored; by irradiation at 285 nm, the characteristic emission of Trp residue in BSA can be traced whereas with excitation at 350 nm, the emission of $Qu(CSA)_2$ can be studied.

Primarily, we kept the concentration of $Qu(CSA)_2$ in aqueous solution constant at 10^{-3} M and adding BSA into the solution largely attenuated the emission intensity of $Qu(CSA)_2$ (Fig. 6A). The solution emission of $Qu(CSA)_2$ was progressively decreased by increasing BSA concentration from 1.5×10^{-5} M to 1.5×10^{-3} M. In principle, the amino groups in the side chains of BSA are the main reacting groups, which compete efficiently with the nitrogen atoms of $Qu(CSA)_2$ for binding with the CSA ligand, rendering a non-emissive quinine base and the observed emission weakening. To evaluate the stoichiometry involved in the reaction, relative emission intensity of I/I_o (I_o and I refer to intensity of the emission peak at 480 nm before and after the addition of BSA, respectively) was therefore plotted against the relative molar ratio of amino groups (583 amino acid[30] per each BSA) to $Qu(CSA)_2$ in Fig. 6B. Here, we observed a fast attenuation of the emission intensity at the beginning, during which increasing BSA concentration from 0 M to 1.5×10^{-4} M (with $[NH]/[Qu(CSA)_2] \sim 87$) already caused 92% intensity loss ($I/I_o = 0.08$). Further increase of BSA in the solution resulted in little difference of the relative intensity. A large amount of amino groups in BSA is therefore responsible for the fast emission quenching at the initial step when only a small amount ($\leq 1.5 \times 10^{-4}$ M) of BSA was loaded in the solution.

The influence of $Qu(CSA)_2$ on the emission of BSA was then evaluated from the emission response of BSA (1.5×10^{-5} M)

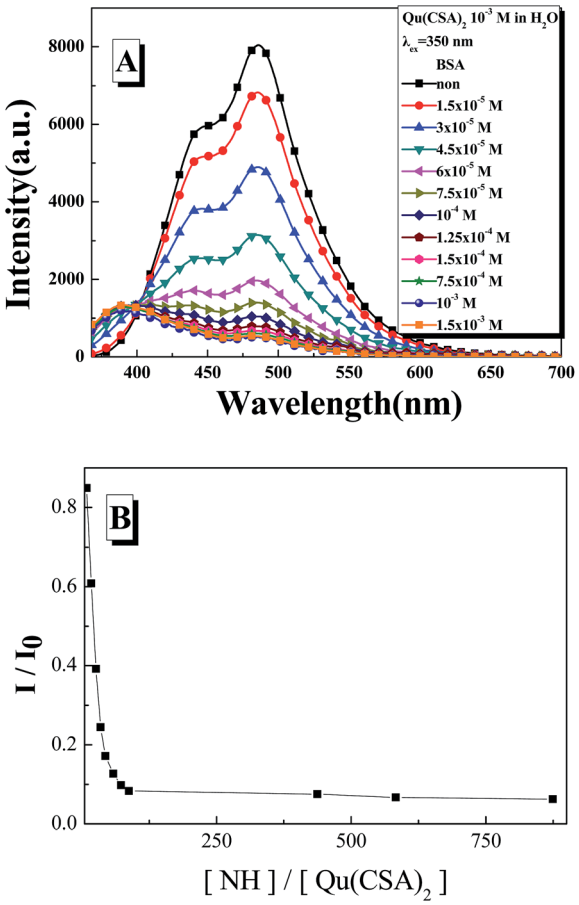

Fig. 6 (A) Emission spectra of the aqueous $Qu(CSA)_2$ (10^{-3} M) solutions containing different amounts of BSA. ($\lambda_{ex} = 350$ nm) and (B) the plot of relative intensity ($I//I_o$, I and I_o are intensity of the peak at 480 nm before and after adding BSA) against the molar ratio of amino groups in BSA relative to $Qu(CSA)_2$.

toward increasing dosage of $Qu(CSA)_2$ in the aqueous solution. At the beginning, emission of BSA was progressively shifted to longer wavelengths and weakened in intensity as the concentration of $Qu(CSA)_2$ was increased from 0 M to 1.5×10^{-5} M (Fig. 7A). However, further increase of $Qu(CSA)_2$ concentration resulted in a reverse intensity gain and a large bathochromic shift (>30 nm) of the peak maxima. As the $Qu(CSA)_2$ concentration reached 4.5×10^{-5} M, aggregate emission of $Qu(CSA)_2$ at 480 nm started to emerge and gradually developed in intensity with increasing $Qu(CSA)_2$ concentration in the solutions. We further increased the $Qu(CSA)_2$ concentration to higher than 3×10^{-4} M and the corresponding emission spectra are summarized in Fig. 7B. Here, the increase of $Qu(CSA)_2$ concentration from 7.5×10^{-4} M to 3×10^{-3} M largely quenched emission of the Trp residue at wavelengths below 400 nm. The weak emission of Trp residue turned into a small shoulder left of the large emission peaks of $Qu(CSA)_2$ at wavelengths over 400 nm. The peptide chain must be subjected to major conformational change at this concentration range.

The change in the secondary structure of BSA by the $Qu(CSA)_2$-induced denaturation can be monitored by far-UV

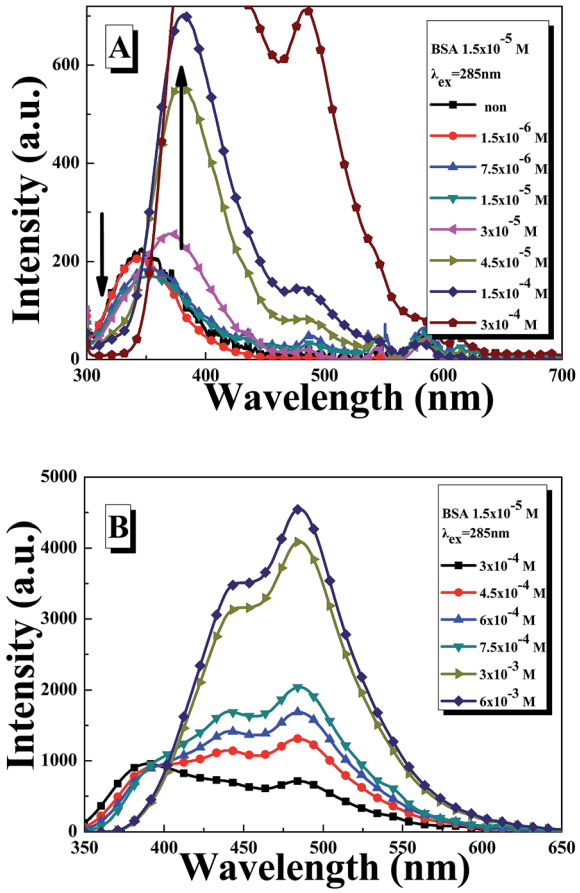

Fig. 7 Emission spectra of the aqueous BSA (1.5×10^{-4} M) solutions containing different amounts of $Qu(CSA)_2$ with concentrations ranged (A) from 0 M to 3×10^{-4} M and (B) from 3×10^{-4} M to 6×10^{-3} M. (λ_{ex} = 285 nm).

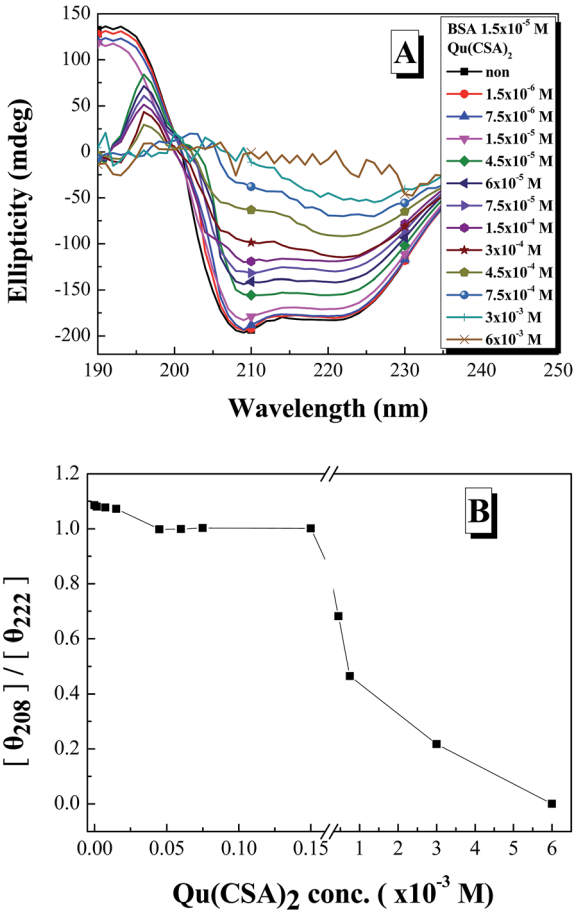

Fig. 8 (A) The CD spectra of the aqueous BSA (1.5×10^{-5} M) solutions containing different amounts of BSA and (B) the ellipticity ratio (θ_{208}/θ_{222}) against the concentration of $Qu(CSA)_2$ in the solutions.

CD. The normal CD spectrum of BSA in aqueous solution showed an α-helix profile with peaks at 208 and 222 nm.[43] When the $Qu(CSA)_2$ concentration is low ($\leq 1.5 \times 10^{-5}$ M), the CD signals remained almost unchanged (Fig. 8A). The ellipticity ratio ($\theta_{208}/\theta_{222}$) was kept constant at *ca.* 1.07. The constant ellipticity ratio suggests that the tertiary structure of BSA, rather than its secondary structure, was perturbed at the low $Qu(CSA)_2$ concentration. Raising the concentration of $Qu(CSA)_2$ to $\geq 4.5 \times 10^{-5}$ M lowered the fraction of α-helical chain of BSA according to the CD signal shift at wavelengths below 200 nm (Fig. 8A) and the lowering of the ellipticity ratio (Fig. 8B). In the intermediate concentration range of $Qu(CSA)_2$ from 4.5×10^{-5} M to 1.5×10^{-4} M), the resolved ellipticity ratios are almost the same at *ca.* 1.00; however, further increase of the $Qu(CSA)_2$ concentration conceivably lowered the ellipticity ratio. At the high $Qu(CSA)_2$ concentration, the protein chains were gradually transformed from helical strands to random coils. No helical strand was detected in the CD spectrum of solution containing 3×10^{-3} M $Qu(CSA)_2$.

As illustrated in Fig. 6A, emission of $Qu(CSA)_2$ progressively decreased with increase of BSA in the solution. The reduced emission intensity is attributed to the reaction between $Qu(CSA)_2$ and BSA where the amino groups in the side chains of BSA attacked the ionic bonds of $Qu(CSA)_2$ resulting in non-emissive quinine base and the observed emission quenching. After reaction, the bulky quinine base intruded into the BSA chains and acted to uncoil the folded peptide chains. In accord with the multistep transition proposed[42] previously, the $Qu(CSA)_2$-induced denaturation process is schematically depicted in Scheme 2. The first step occurred at the low $Qu(CSA)_2$ concentration ($\leq 1.5 \times 10^{-5}$ M), during which no significant change in the secondary structure was involved as indicated by the CD spectra. Nevertheless, attenuation in the emission intensity of BSA implies that there exists a transition involving rearrangement of the tertiary structure. Possibly, the intruding quinine bases acted to separate the peptide domains and opened the inter-domain hydrophobic pocket. Within the opened hydrophobic pocket, the emissive Trp residue was more exposed to, and thus more sensitive to, the surrounding polar media. Emission of Trp residue was therefore shifted to longer wavelengths and became less intense due to the solvent relaxation process promoted by the polar media.

The second stage occurred at $\sim 3 \times 10^{-4}$ M $Qu(CSA)_2$ and was distinguished by the reverse emission enhancement and *ca.* 7% loss in the ellipticity ratio. Although part of the secondary structures may already be damaged by $Qu(CSA)_2$, the molten-

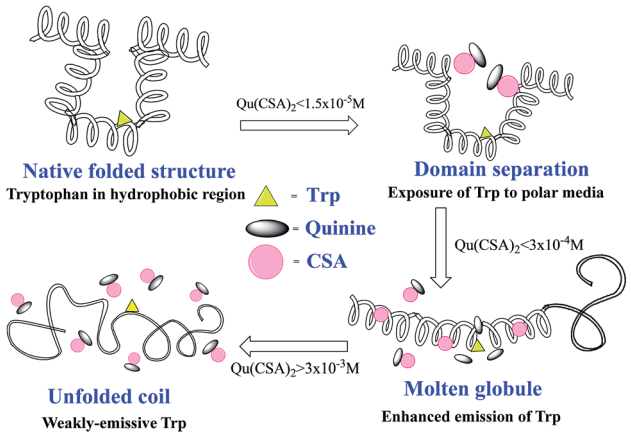

Scheme 2 Proposed mechanism for fluorescent probing of the $Qu(CSA)_2$-induced BSA unfolding process.

globule state still offers additional hydrophobic sites for the quinine base. The intra-domain contacts may become loose due to the swelling effect, which facilitates approaches of the intruding quinine bases to nearby range of the Trp residues inside the domains. In close vicinities, the bulky quinine bases sterically rigidified the Trp residue and effectively blocked the non-radiative decay process of the excited Trp unit resulting in large emission enhancement of the Trp residue (*cf.* Fig. 7). The intimate contact also reinforced the intermolecular π–π stacking interactions between the quinoline ring of the quinine base and the indole ring of the Trp residue, thus continually shifting the emission to longer wavelengths as the $Qu(CSA)_2$ concentration was increased.

Finally, when excess $Qu(CSA)_2$ ($\geq 3 \times 10^{-3}$ M) was added into the aqueous solution of BSA, the secondary structures of the BSA chains were mostly damaged and transformed into random coils. At this stage, Trp residue in the unfolded chains was fully exposed to the polar environment and its emission was largely weakened by the extensive solvent relaxation process. Excess $Qu(CSA)_2$ complexes loaded in the solutions therefore emitted intensely at wavelengths over 400 nm.

Conclusion

In this study, ionic complexes of $Qu(CSA)_x$ were conveniently prepared by complexing quinine with different amounts of CSA. Among all complexes, $Qu(CSA)_2$ was chosen as a model system for study and the result suggested that it is an AIE-active ionic luminogen due to the effective rotational restriction imposed by the bulky CSA. Without the bulky component, the ionic complex $Qu(HCl)_2$ is a normal luminogen without AIE activity.

The ionic complex of $Qu(CSA)_2$ is a convenient multiple luminescent sensor responsive to acid, base, counter anions, and the blood protein BSA. The responses of $Qu(CSA)_2$ towards different additives can be attributed to the ionic bonds of $Qu(CSA)_2$. All interactions of the analytes applied above tend to rupture the ionic bonds of $Qu(CSA)_2$, generating non-emissive quinine species and resulting in the observed emission intensity reduction.

Besides being luminescent sensor, the ionic complex of $Qu(CSA)_2$ also serves as a denaturant effective in uncoiling the folded chains of BSA. The unfolding process of BSA was therefore evaluated by combined results from the emission and the CD spectra. A three-step process, involving the rearrangement of the tertiary structure, the formation of molten globule, and the collapse of secondary structure, was therefore proposed in this study. Emission responses of the Trp residue and the added $Qu(CSA)_2$ were correlated with the three-step unfolding process.

Acknowledgements

We appreciate the financial support from the Ministry of Science and Technology, Taiwan, under the contract no. MOST102-2221-E-110-084-MY3 and 104-2221-E-110-050.

References

1 J. Luo, Z. Xie, J. W. Y. Lam, L. Cheng, H. Chen, C. Qiu, S. Kwok, X. Zhan, Y. Liu, D. Zhu and B. Z. Tang, *Chem. Commun.*, 2001, 1740.
2 B. Z. Tang, X. Zhan, G. Yu, P. P. S. Lee, Y. Liu and D. Zhu, *J. Mater. Chem.*, 2001, **11**, 2974.
3 Y. Hong, J. W. Y. Lam and B. Z. Tang, *Chem. Commun.*, 2009, 4332.
4 D. Ding, K. Li, B. Liu and B. Z. Tang, *Acc. Chem. Res.*, 2013, **46**, 2441.
5 Z. Zhao, J. W. Y. Lam and B. Z. Tang, *J. Mater. Chem.*, 2012, **22**, 23726.
6 M. Wang, G. Zhang, D. Zhang, D. Zhu and B. Z. Tang, *J. Mater. Chem.*, 2010, **20**, 1858.
7 Z. Zhao, J. W. Y. Lam and B. Z. Tang, *Soft Matter*, 2013, **9**, 4564.
8 *Aggregation-Induced Emission: Fundamentals*, ed. A. Qin and B. Z. Tang, John Wiley & Sons, Ltd, NY, 2013.
9 J. Mei, Y. Hong, J. W. Y. Lam, A. Qin, Y. Tang and B. Z. Tang, *Adv. Mater.*, 2014, **26**, 5429.
10 H. Wang, E. Zhao, J. W. Y. Lam and B. Z. Tang, *Mater. Today*, 2015, **18**, 365.
11 J. Mei, N. L. C. Leung, R. T. K. Kwok, J. W. Y. Lam and B. Z. Tang, *Chem. Rev.*, 2015, **115**, 11718.
12 Z. Li, Y. Dong, B. Mi, Y. Tang, M. Häussler, H. Tong, Y. Dong, J. W. Y. Lam, Y. Ren, H. H. Y. Sung, K. S. Wong, P. Gao, L. D. Williams, H. S. Kwok and B. Z. Tang, *J. Phys. Chem. B*, 2005, **109**, 10061.
13 J. Chen, C. C. W. Law, J. W. Y. Lam, Y. Dong, S. M. F. Lo, I. D. Williams, D. Zhu and B. Z. Tang, *Chem. Mater.*, 2003, **15**, 1535.
14 J. Achanl, A. O. Talisuna, A. Erhart, A. Yeka, J. K. Tibenderana, F. N. Baliraine, P. J. Rosenthal and U. D'Alessandro, *Malar. J.*, 2011, **10**, 144.
15 W. H. Melhuish, *J. Phys. Chem.*, 1961, **65**, 229.
16 J. E. Sabol and M. G. Rockley, *J. Photochem. Photobiol., A*, 1987, **40**, 245.
17 J. N. Demes and G. A. Graby, *J. Phys. Chem.*, 1971, **75**, 991.
18 W. H. Melhuish, *J. Phys. Chem.*, 1960, **62**, 762.

19 S. G. Schulman, R. M. Threatte, A. C. Capomacchia and W. L. Paul, *J. Pharm. Sci.*, 1974, **63**, 876.
20 D. A. Barrow and B. R. Lentz, *Chem. Phys. Lett.*, 1984, **104**, 163.
21 J. Eisenbrand and M. Z. Raisch, *Anal. Chem.*, 1961, **179**, 352.
22 D. Pant, U. C. Tripathi, G. C. Joshi, H. B. Tripathi and D. D. J. Pant, *J. Photochem. Photobiol., A*, 1990, **51**, 313.
23 C. A. Chou, R. H. Chien, C. T. Lai and J. L. Hong, *Chem. Phys. Lett.*, 2010, **80**, 501.
24 J. B. Birks, *Photophysics of Aromatic Molecules*, Wiley, London, 1970.
25 J. Chen, C. C. W. Law, J. W. Y. Lam, Y. Dong, S. M. Lo, I. D. Williams, D. Zhu and B. Z. Tang, *Chem. Mater.*, 2003, **15**, 1535.
26 T. Lai, R. H. Chien, S. W. Kuo and J. L. Hong, *Macromolecules*, 2011, **44**, 6546.
27 C. M. Yang, Y. W. Lai, S. W. Kuo and J. L. Hong, *Langmuir*, 2012, **28**, 15725.
28 Y. Moriyama, D. Ohta, K. Hadiya, Y. Mitsui and K. J. Takeda, *J. Protein. Chem.*, 1996, **15**, 265.
29 X. M. He and D. C. Carter, *Nature*, 1992, **358**, 209.
30 Y. Z. Zhang, B. Zhou, X. P. Zhang, P. Huang, C. H. Li and Y. Liu, *J. Hazard. Mater.*, 2009, **163**, 1345.
31 C. Tanford, K. Kawahara and S. Lapanje, *J. Am. Chem. Soc.*, 1967, **89**, 729.
32 J. C. Lee and S. N. Timasheff, *Biochemistry*, 1974, **13**, 257.
33 S. De, A. Girigoswami and S. Das, *J. Colloid Interface Sci.*, 2005, **285**, 562.
34 D. Kelley and D. J. McClements, *Food Hydrocolloids*, 2003, **17**, 73.
35 S. L. Deng, T. S. Hsiao, K. Y. Shih and J. L. Hong, *J. Photochem. Photobiol., B*, 2014, **138**, 134.
36 T. Singh, P. Bharmoria, M. Morikawa, N. Kimizuka and A. Kumar, *J. Phys. Chem. B*, 2012, **116**, 11924.
37 S. M. Yarmoluk, D. V. Kryvorotenko, A. O. Balanda, M. Y. Losytskyy and V. B. Kovalska, *Dyes Pigm.*, 2001, **51**, 41.
38 M. K. Santra, A. Banerjee, S. S. Krishnakumar, O. Rahaman and D. Panda, *Eur. J. Biochem.*, 2004, **271**, 1789.
39 R. B. Singh, S. Mahanta, A. Bagchi and N. Guchhait, *Photochem. Photobiol. Sci.*, 2009, **8**, 101.
40 H. Jun, Y. H. Soo, S. Y. Seung, C. Kang and M. Suh, *Chem. Lett.*, 2004, **33**, 690.
41 S. Gorinstein, I. Goshev, S. Moncheva, M. Zemser, M. Weisz, A. Caspi, I. Libman, H. T. Lerner, S. Trakhtenberg and O. J. Martin-Belloso, *J. Protein. Chem.*, 2000, **19**, 637.
42 Y. Hong, C. Feng, Y. Yu, J. Liu, J. W. Y. Lam, K. Q. Luo and B. Z. Tang, *Anal. Chem.*, 2010, **82**, 7035.
43 P. J. Rossky, *Proc. Natl. Acad. Sci. U. S. A.*, 2008, **105**, 16825.

